

Coal fouling characteristic to deposit probe with different temperatures under the gasification condition

Hueon Namkung*, Tae-Jin Kang*, Li-Hua Xu**, Young-Shin Jeon*, and Hyung-Taek Kim*[†]

*Division of Energy Systems Research, Graduate School, Ajou University,
Wonchon-dong, Yeongtong-gu, Suwon 443-749, Korea

**Plant Engineering Center, IAE, Wonchon-dong, Yeongtong-gu, Suwon 443-749, Korea

(Received 1 July 2011 • accepted 16 August 2011)

Abstract—Coal gasification was carried out to verify the coal fouling characteristic in a drop tube furnace (DTF). Four pulverized coal samples, in the range of bituminous and sub-bituminous, were used. To analyze the fouling characteristic by different temperature of deposit probe, a two-stage deposit probe was used in the experiment. Ash deposition rate was at upper deposit probe higher than at lower one. The X-ray fluorescence (XRF) results indicated that coal fouling included acid minerals such as SiO_2 and Al_2O_3 at upper deposit probe more than that at lower deposit probe. The results of X-ray diffraction (XRD) and scanning electron microscopy (SEM) indicated that the fouling particles at high deposit temperature were agglomerated more than those at low deposit temperature. And the convective heat transfer efficiency was reduced by ash deposition on probe. Especially, the convective heat transfer coefficient substantially declined with small particle size of fouling and Fe_2O_3 , CaO , and MgO .

Key words: Fouling, Gasification, Convective Heat Transfer Coefficient, Minerals

INTRODUCTION

Fossil fuel technologies are gradually claiming to be cleaner and more effective. So gasification technology has become a technical issue as a representative clean coal technology to produce energy [1]. Gasification technology such as integrated gasification combined cycle (IGCC) can not only satisfy future energy demand but also provide environmentally acceptable options among the candidate power generation technologies [2,3]. However, IGCC plant demonstration claims that major obstacle during the operation is caused by ash deposition. Generally, the amount of deposit-forming ash material ranges between 10 and 25% ash content of the feed coal by weight. Particulate fouling is defined as the accumulation of particles on a heat transfer surface that form an insulating layer, which reduces the rate of heat transfer and can lead to operation failure as has been reported by many researchers [4-6]. The composition and properties of these solid products are dependent on the coal types and technological processes used in gasifier. Fly ash is produced according to the gasification temperature (entrained bed gasifier, $<1,500^\circ\text{C}$) [7] and it is generated from various inorganic and organic constituents present in feed coals. The composition and properties of fly ash have been briefly characterized by many researchers [8-10]. The phase and mineral composition of fly ash are introduced briefly.

(1) Inorganic constituent - comprising non-crystalline (amorphous) matter, namely different glassy particles, and crystalline (mineral) matter such as crystals, grains and aggregates of various minerals

(2) Organic constituent - composed of char materials (slightly changed, semi-coked and coked particles) and organic minerals

(3) Fluid constituent - comprising liquid (moisture), gas and gas-liquid inclusions associated with both inorganic and organic matter

According to the nature of coal, mineral matters experience different chemical and physical transformations in the gasification process. Mineral materials experience fragmentation, fusion, and chemical reactions prior to solidification, which defines the characteristics of the resultant ash. Being associated with other mineral particles, minerals are also likely to undergo coalescence during gasification.

Coalescence of dissimilar minerals can result in the formation of lower melting eutectics by the original mineral composition, and increasing ash deposition propensity. Fouling phenomenon on heat transfer area is initiated by the deposition of a thin layer of material of condensed vapors [11,12]. The composition of this material is typically high in alkaline earth and alkali minerals which can be easily vaporized.

And they may react with sulfates. The deposition of inorganic material during coal gasification or combustion includes five general mechanisms including inertial impaction, thermophoresis, condensation, eddy deposition and chemical reaction [13,14].

Ash deposition is related to the mineral composition in coal. And also, ash deposition phenomenon influences on heat transfer efficiency of gasification system. The purpose of this study is to investigate the coal fouling behavior through the experiments in drop tube furnace (DTF), in which behavior of coal particle in gasification condition can be investigated experimentally.

EXPERIMENTAL SECTION

1. Preparation of Coal Samples

Four different coal samples are chosen for the experiments, which represents a wide range of mineral contents of bituminous and sub-bituminous coal.

[†]To whom correspondence should be addressed.
E-mail: htkim@ajou.ac.kr

Table 1. Basic analysis of coal samples in the experiments

		Minmetal	Centennial	Taldinsky	MHU
Proximate analysis (dry-basis, wt%)	V.M	29.01	30.05	32.32	46.3
	F.C	61.57	53.48	55.67	48.71
Ultimate analysis (ash-free base, wt%)	C	85.06	83.04	79.59	59.71
	H	4.75	5.16	4.74	4.61
	O	8.48	9.56	13.53	33.33
	N	0.79	1.69	1.94	1.31
	S	0.92	0.55	0.2	1.04
Heating value (HHV)	kcal/kg	6,601	6,534	5,954	5,706

Table 2. Chemical components and fusion temperature of ash in coal samples

		Minmetal	Centennial	Taldinsky	MHU
Inorganic analysis (wt%)	SiO ₂	42.9	62.1	42.2	29.2
	Al ₂ O ₃	11.2	15.5	14.1	9.26
	Fe ₂ O ₃	19.7	5.89	24.9	46.2
	CaO	17.3	1.69	9.15	8.62
	MgO	0.34	0.07	0.33	0.162
	Na ₂ O	0.06	0.03	0.07	-
	K ₂ O	4.18	8.49	4.67	3.31
	TiO ₂	4.32	6.3	4.59	3.17
Ash fusion temp. (°C)	IT	1250	>1550	1300	1250
	ST	1270	>1550	1320	1270
	HT	1290	>1550	1340	1290
	FT	1310	>1550	1360	1310

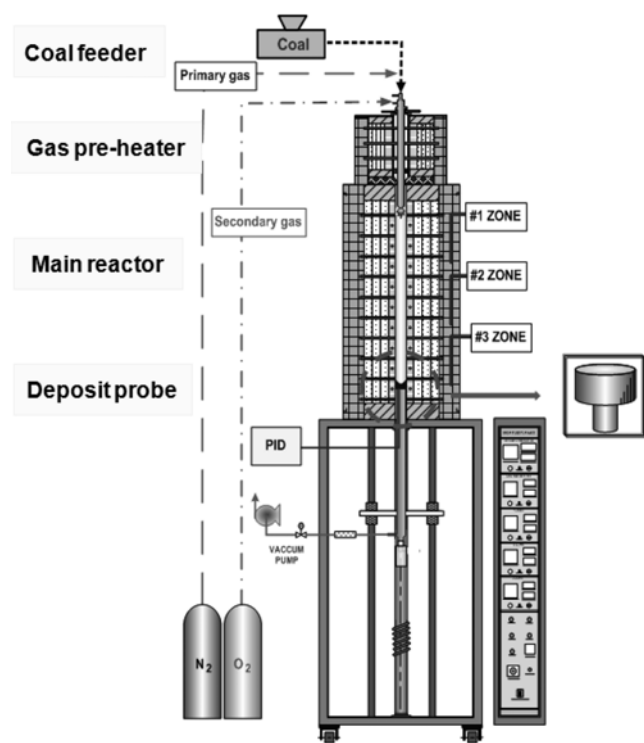
Original coal samples were dried and crushed in a fan type disk mill, and then were separated into the size range under 75 μm by electromagnetic shaker. Basic analysis of coal samples is illustrated in Table 1 as the result of proximate and ultimate analysis. The chemical compositions of coal ash are also given in Table 2, in with chemical elements of SiO₂, Al₂O₃, Fe₂O₃, CaO, MgO, Na₂O, K₂O and TiO₂ assigned as major components of the ash. The deposition behavior of coal samples is studied by using the DTF and deposit probe as shown in Fig. 1.

2. Experimental Apparatus

DTF has a feature which can simulate the environment of the coal gasifier. The system mainly consists of coal sample injector, pre-heater, main tube furnace reactor and deposit probe. The temperature of the main reactor is set to 1,300 °C. The temperature zone is divided into three zones to easily maintain reactor temperature and its temperature control by proportional - integral - derivative (PID) system. Pulverized coal is fed at the top of DTF by using screw feeder with nitrogen gas (primary gas). And then injected coal particles react with concentric oxygen gas (secondary gas) in the DTF. During each experiment, coal sample is continuously fed for 10 minutes to the DTF. The coal feeding rate is 0.4-0.6 g/min and ratio of O₂/coal is set to 0.9. The pre-heater is set to 1,000 °C to prevent sudden thermal expansion of flue gas including coal. Coal particles transform through devolatilization and char burning by being heated and passed before ash formation and then collected on the deposit probe. The deposit probe is vertically inserted into the end of lowest furnace section. The probe position vertically moves up and down to adjust its surface temperature by using mechanical elevator. The surface temperature of probe is changed from 500 °C to 1,000 °C during the experiment.

Sampling deposit probe is made of two stages where top stage is called as 1st layer and bottom stage is called as 2nd layer as shown in Fig. 2. The 1st layer always has higher temperature condition than the 2nd layer because the 2nd layer is close to the reactor outlet. The height between the 1st and 2nd layer is controlled by probe supporter whose length is 1, 2 and 3 cm. The probe supporter can accommodate the temperature control between the 1st and 2nd layer. When the length of the probe supporter is 1 cm, there is 100 °C temperature difference between the 1st and 2nd layer. The reason for using two stages deposit probe is that it is easier to investigate coal fouling phenomenon in an actual gasification process. Once the experiment is carried out, two ash samples can be contemporarily gotten at the one experimental condition.

Pulverized coal samples are injected into DTF under gasifica-

**Fig. 1. Schematic of the entire experimental facility and deposit probe.**

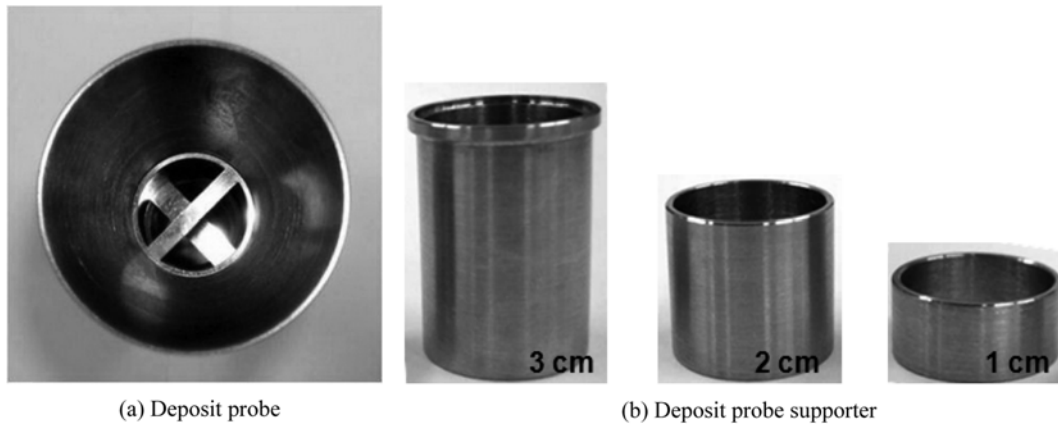


Fig. 2. Photograph of deposit probe.

tion condition. The ash particles are deposited onto sample collector by impacting and agglomerating effect; deposited samples of ash are analyzed to determine their characteristics such as the fouling amount, composition and shapes of deposited ash.

3. Evaluation of Convective Heat Transfer Coefficient

Generally, convective heat transfer coefficient is reduced by fouling phenomenon. Reduction of convective heat transfer coefficient by fouling phenomenon is calculated with different coal samples and deposition temperature to analyze the effect of ash deposition on deposit probe.

Widely used, basic equation for convective heat transfer coefficient k can be presented as follows.

$$k = \psi k_i \quad (1)$$

where

ψ : thermal effectiveness number

k_i : convective heat transfer coefficient for ideal conditions, ($\text{W}/\text{m}^2 \text{K}$)

Convective heat transfer coefficient for ideal conditions is $2,840 \text{ W}/\text{m}^2 \text{K}$ in gases state [15]. It is recommended for use in designing heat-transfer equipment. Thermal effectiveness number (ψ) allows incorporating into calculations of some diverse factors affecting heat transfer intensity. If there is no ash deposition on heat transfer surface, thermal effectiveness number doesn't decrease. The principal factors that influence on ψ are [16]:

- a) fouling on heat transfer surfaces,
- b) non-uniform flue gases flow distribution over convective bundles which are situated in ducts of significant dimensions and complicated geometry,
- c) corrosion of tubing material.

The influence of fouling on heat transfer can be calculated by means of thermal effectiveness number (ψ) for various forms of deposits and their properties. However, it is necessary to know the shape, sizes and properties of deposits. In fact, these values can hardly be predicted and must be investigated. To avoid problems, a simplified method of characterizing the effect of fouling on heat transfer was proposed in Ref. [16,17] and is based on the same set of independent variables like in case of Eq. (2). The thermal effectiveness number can be expressed like following:

- In case of staggered tube banks

$$\psi = 0.46 \sigma^{-0.111} \left(\frac{w}{w_b} \right)^{0.056} \left(\frac{R_{0.03}}{R_{0.03b}} \right)^{0.09} \left(\frac{T}{T_b} \right)^{-0.138} c_m^{-0.394} \quad (2)$$

For ash deposition experiment, the 1st and 2nd deposit layer were installed like cross type. Therefore, the equation for thermal effectiveness number was chosen in case of staggered tube banks. However, some parameters were modified because they can't be directly adapted in this experiment. The modified equation is expressed in Eq. (3).

$$\psi = 0.46 A^{-0.111} \left(\frac{w}{w_b} \right)^{0.056} \left(\frac{R_{0.03}}{R_{0.03b}} \right)^{0.09} \left(\frac{T}{T_b} \right)^{-0.138} c_m^{-0.394} \quad (3)$$

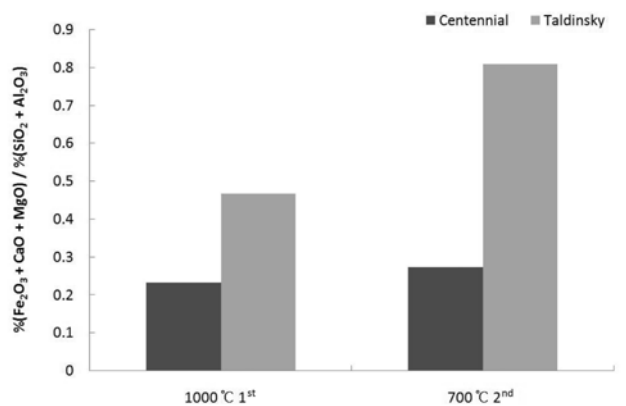
- 1) A =deposit area
- 2) w/w_b =relative mean velocity of the flue gas on the deposit probe
- 3) $R_{0.03}/R_{0.03b}$ =relative ash particle-size distribution [$R_{0.03}$ - percentage of particles bigger than $30 \mu\text{m}$, %]
- 4) T/T_b =relative mean temperature of the flue gas on the deposit probe
- 5) c_m =chemical constitution of fly ash represented as B/A , [% ($\text{Fe}_2\text{O}_3 + \text{CaO} + \text{MgO}$)/% ($\text{SiO}_2 + \text{Al}_2\text{O}_3$)]
- 6) The basic values have been chosen as: $w_b = 1 \text{ m/s}$, $R_{0.03b} = 24.5\%$ and $T_b = 373 \text{ K}$.

RESULTS AND DISCUSSION

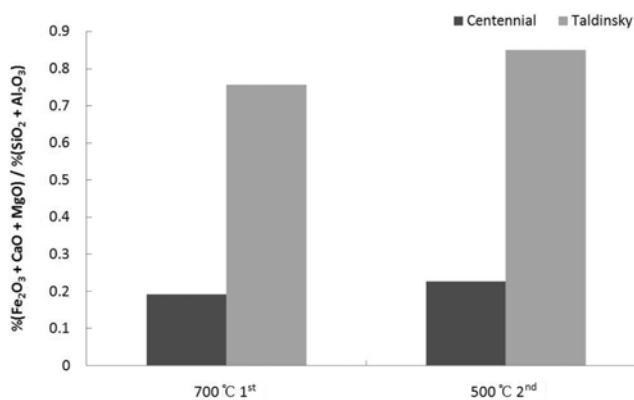
1. Deposit Amounts and Chemical Characteristic of Fouling

X-ray fluorescence (XRF) results of deposited fouling samples under gasification condition are presented in Fig. 3. The total quantity of alkali is not necessary to explain fouling potential. Fouling phenomenon is well related to the quantity of "active alkalis" [18]. Organically bonded alkali and alkaline-earth minerals have the potential to form very reactive species in the gasification/combustion area as transient elements or compounds. Fe_2O_3 , CaO , and MgO are fluxing agents in the fouling phenomenon because they make a low melting point of coal minerals. From the XRF result, % ($\text{Fe}_2\text{O}_3 + \text{CaO} + \text{MgO}$)/% ($\text{SiO}_2 + \text{Al}_2\text{O}_3$) ratio is higher in the fouling deposit of the 2nd layer than that of the 1st layer.

Commonly, fouling is initiated by the deposition of condensed vapor materials which make a thin layer. The initial deposit layers



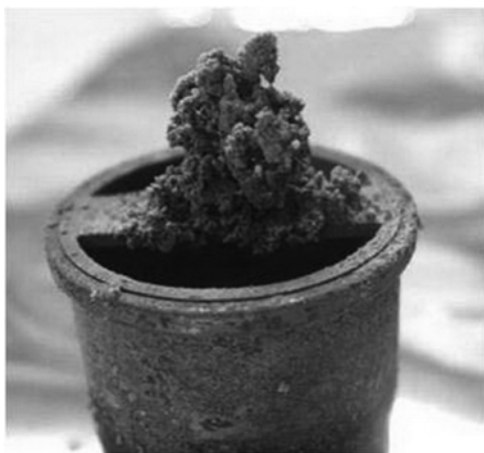
(a) Chemical composition of coal fouling at 1st layer (1000 °C) and 2nd layer (700 °C)



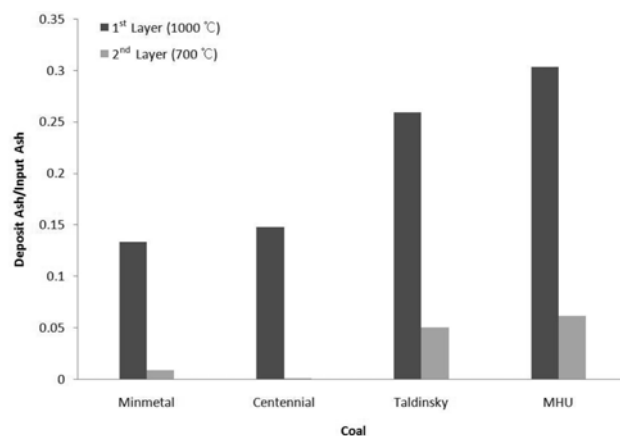
(b) Chemical composition of coal fouling at 1st layer (700 °C) and 2nd layer (500 °C)

Fig. 3. Comparison of fouling chemical composition on 1st and 2nd layer by XRF.

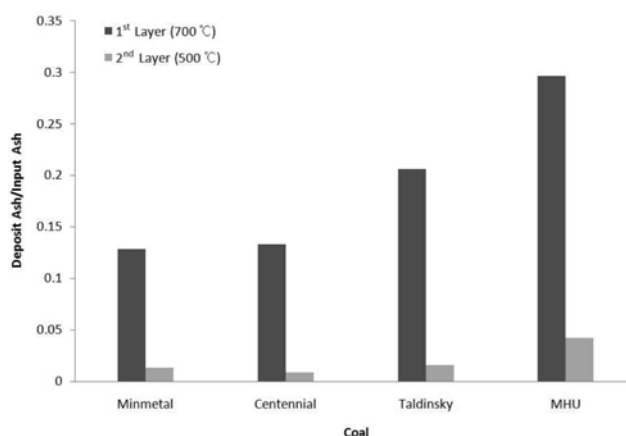
may provide a sticky surface to trap particles by inertial force which isn't sticky. In addition, the initial layers may provide fluxing materials that will cause larger particles to be melted. Alkali and alka-



(a) Deposit fouling on 1st layer (700 °C)



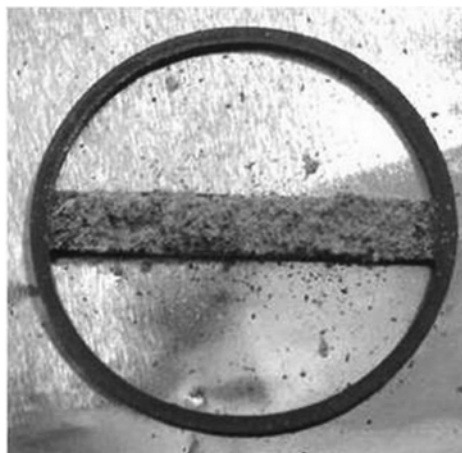
(a) Amounts of ash deposition on 1st layer (1000 °C) and 2nd layer (700 °C)



(b) Amounts of ash deposition on 1st layer (700 °C) and 2nd layer (500 °C)

Fig. 5. Comparison of amounts of ash deposition on 1st and 2nd layer.

line earth minerals provide a binding matrix for acid mineral such as alumina and silica, and ash particles to fuse together and build



(b) Deposit fouling on 2nd layer (500 °C)

Fig. 4. Picture of the deposited fouling on probe.

up on deposit surface [12].

Deposited fouling on the 1st deposit layer includes many acid minerals such as silica and alumina because the initial layer of alkali and alkaline earth minerals provides acid minerals with a binding matrix to be agglomerated and then fouling can grow up. However, deposited fouling of the 2nd layer cannot include many acid minerals such as alumina and silica because agglomerated fouling deposit on the 1st layer shields the 2nd layer and disturbs the approach of acid minerals at the 2nd layer. For this reason, even though alkali and alkaline earth minerals which have sticky force can easily deposit on the layer, fouling on the 2nd layer cannot grow up by attachment of acid minerals. The pictures of deposit fouling on the 1st and 2nd

layer are shown in Fig. 4. Deposit amounts of fouling on the 1st layer and 2nd layer are illustrated in Fig. 5. Deposit amounts of fouling are abundant at the 1st layer more than at the 2nd layer as in Figs. 4 and 5.

And also their deposit amounts on the 1st layer are a little more plentiful at 1,000 °C than at 700 °C, because coal minerals can easily exist as molten phase to adhere on deposit probe at high deposition temperature.

2. Coal Fouling Size and Shape by Deposition Temperature

From scanning electron microscopy (SEM) and X-ray diffractometry (XRD), the fouling particle sizes by changing temperature of deposit probe are compared in Fig. 6 and Fig. 7. Fouling sam-

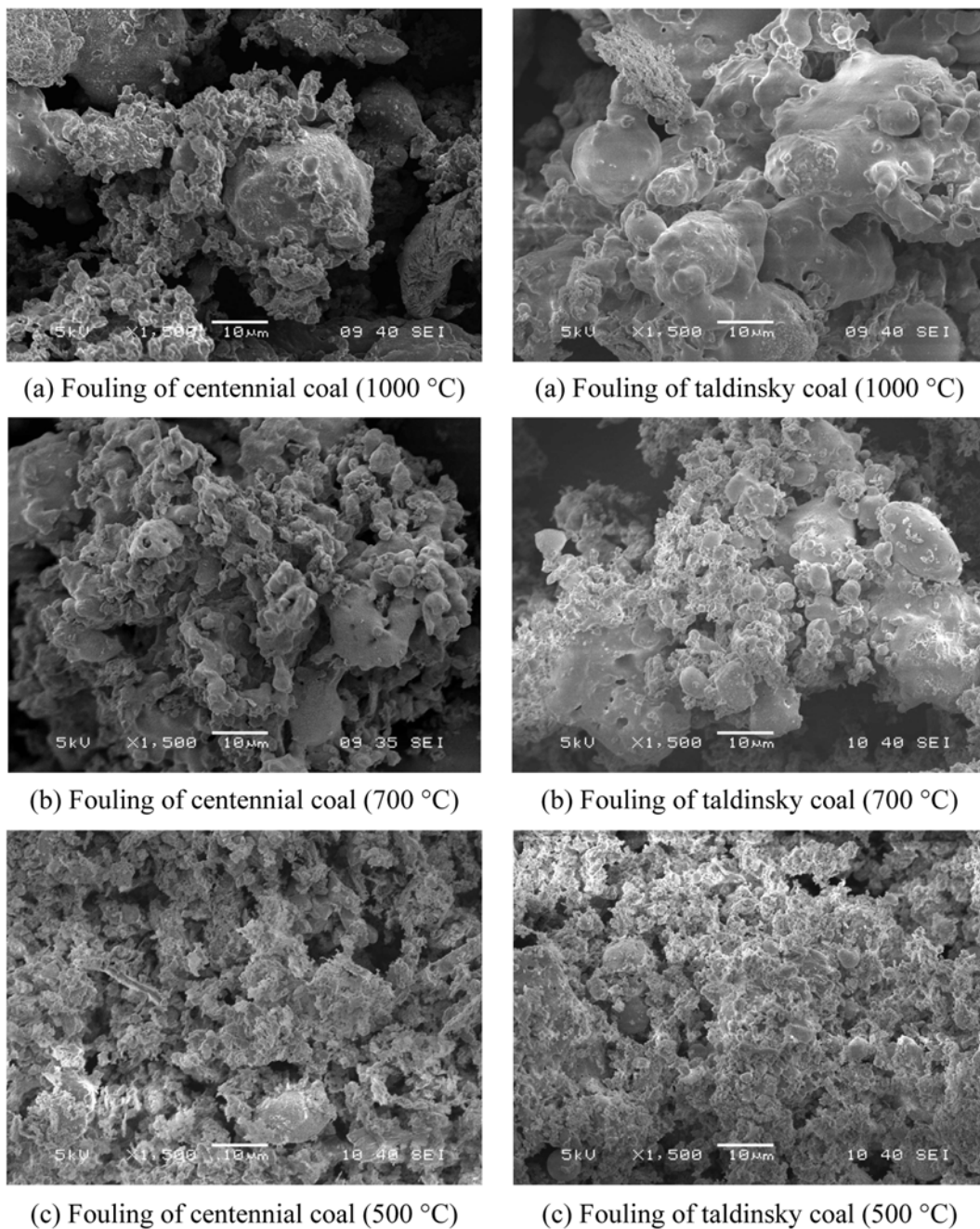


Fig. 6. Fouling particle shape by temperature difference of deposit probe.

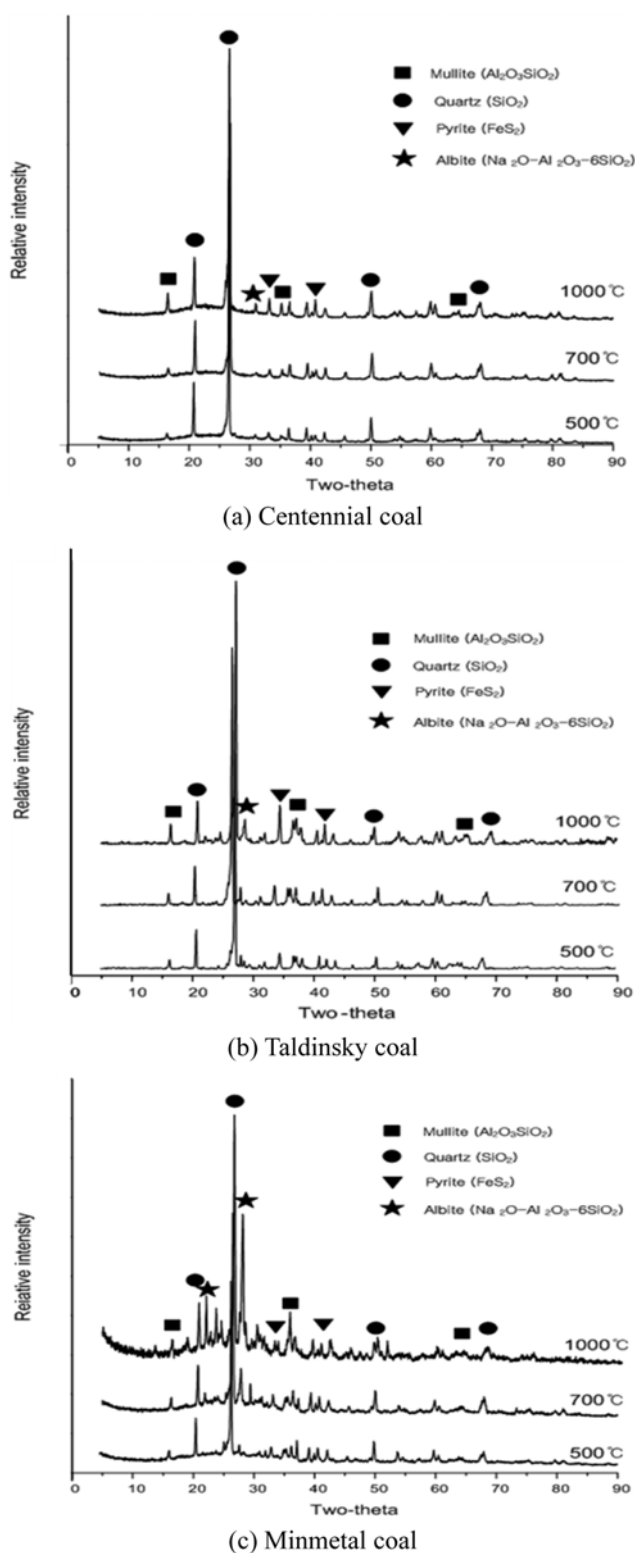


Fig. 7. XRD pattern of fouling by temperature difference of deposit probe.

Table 3. Particle size difference of fouling by shaking period

	Centennial #1 (2 hours)	Centennial #2 (4 hours)	Centennial #3 (6 hours)	Centennial #4 (8 hours)
Average size of coal fouling particle (μm)	68.14	54.80	47.75	47.62

ples on the 1st layer are analyzed to correctly verify their characteristics. Fouling characteristics of Centennial and Taldinsky coal are analyzed with different particle sizes.

Fouling particle size of Taldinsky coal is bigger than that of Centennial coal as in Fig. 6, because of CaO, MgO and Fe₂O₃ minerals. From Table 2, it is shown that Taldinsky coal has more CaO, MgO and Fe₂O₃ minerals than Centennial coal. Fouling of Taldinsky coal can be easily melted and made eutectic compound more easily than that of Centennial coal. And the particle size of coal fouling is bigger at high temperature than that at low temperature as illustrated in Fig. 6 and Fig. 7. The shape of the coal fouling deposit is smooth with increasing of alkali and alkaline-earth mineral contents and temperature. Especially, the iron rich particle has spherical morphology because Fe mineral acts as the main flux agent on the fouling surface.

Peaks resulting from the dominant minerals, such as quartz, mullite, albite and pyrite, are visible in the XRD pattern obtained from the deposit fouling. It means that their minerals are abundant in coal fouling. And most particle sizes of coal fouling with eutectic compound at the high temperature are bigger than those of low temperature. The reason is that melting point of eutectic compound is lower than that of singular compound such as mullite, quartz and so on. Although the main compound of mullite is 3Al₂O₃·2SiO₂ which has high melting temperature, most eutectic compounds are made of Na, K, Fe and Mg elements and then they can be melted at low temperature. Particle size of albite (Na₂O·Al₂O₃·6SiO₂) compound observed in XRD is big at high temperature because albite exists as a eutectic compound. For this reason, fouling particle sizes of eutectic compounds at high temperature are relatively bigger than those at low temperature. Fe elements which occupy many portions among alkali and alkaline minerals are verified as FeS₂ in XRD. Fouling particle sizes of most eutectic compounds including Fe mineral at high temperature are relatively bigger than those at low temperature. The lowest temperature melting phase in fly ashes concerns the presence of iron particles containing oxygen and sulfur. Their FeO-FeS system has a eutectic point of 930 °C [19]. Under reducing condition, iron-rich materials are derived from the iron-rich minerals such as pyrite, siderite, and iron sulphates [20]. Especially, the formation of iron sulfides is not related to condensation of pyrrhotite from flue gas, but mostly likely to be the result of reaction between gaseous hydrogen sulfide and Fe glass exudation formed on the fly ash surfaces [21].

The accurate fouling particle size of Centennial, Taldinsky and MHU coal is analyzed by deposit temperature and coal types. The fouling of Centennial coal is deposited at temperature of 1,000 °C, 700 °C and 500 °C on the 1st layer. And the fouling of Taldinsky and MHU coal is deposited at 700 °C, respectively, on the 1st layer. To accurately analyze fouling particle size, physically attached particles are firstly removed by using an electromagnetic shaker. The fouling of Centennial coal is shaken for 2, 4, 6, and 8 hours, respectively, to find the proper shaking period. And the result is presented

Table 4. Fouling particle size by coal type and deposit temperature difference

		Centennial	Taldinsky	MHU
Deposited temperature (1,000 °C)	Mean value of fouling particle size (μm)	47.75	-	-
	Percentage of particles bigger than 30 μm (%)	68.12	-	-
Deposited temperature (700 °C)	Mean value of fouling particle size (μm)	31.05	67.35	171.69
	Percentage of particles bigger than 30 μm (%)	51.12	76.52	87.35
Deposited temperature (500 °C)	Mean value of fouling particle size (μm)	20.95	-	-
	Percentage of particles bigger than 30 μm (%)	37.62	-	-

on Table 3.

From result of analysis, the fouling particle size is almost the same after 6 hours. It means that the period of 6 hours is an appropriate period to separate physically attached particles. Accordingly, all samples are shaken for 6 hours before the fouling particle size analysis. Average particle size of each sample and percentage of particle size which is bigger than 30 μm are shown in Table 4. The particle size of deposited Centennial coal fouling at temperature of 1,000 °C is the biggest among the samples. It means that acid minerals including alkali minerals easily become eutectic compounds at high temperature and can be made of big particles.

From analysis result of particle size with different coal types, it is evaluated that the average particle size of MHU coal fouling is the biggest among coal types. MHU coal has much Fe content, compared to other coal. Due to its high content, Fe mineral agglomerates ash particles to become big particles and is expected to be the main fluxing species in ash deposition.

3. The Variation of Convective Heat Transfer Coefficient by Ash Deposition

The calculations of convective heat transfer in boiler technology are conducted by empirical correlations obtained in standard conditions, but there is no empirical result obtained from gasification condition. Ash sintering on heat exchangers causes a decrease of heat transfer capacity, difficulty in cleaning the deposited ash and, occasionally, it could reach mechanical failure in the heat exchangers [22]. Generally, the convective heat transfer coefficient of the flue gas is decreased due to the ash deposition. It is necessary to investigate convective heat transfer coefficient decrease by ash deposition.

In this study, a variation of convective heat transfer coefficient by fouling phenomenon is observed under the gasification condition. The DTF experiments are carried out under different condition of coal types and temperature difference of deposit surface. As mentioned, if the fouling is not generated, thermal effective number (ψ) is 1. Otherwise, ψ is decreased. The thermal conductivity of the ash is very low and any ash build-up on the tubes effectively insulates the tube [23]. It has an effect on decrease of convective heat transfer coefficient. For this reason, the process efficiency on heat transfer surface is decreased by fouling phenomenon. Therefore, the investigation of the fouling influence on heat transfer is considered important.

Fouling samples on the 1st layer are used to calculate the convective heat transfer coefficient. The thermal effective number (ψ) is calculated from obtained parameter values on Table 5. Table 6 is shown for the value of thermal effective number by different coal types and temperature. The thermal effectiveness numbers reduce

Table 5. The parameter values for thermal effectiveness number

		Deposited temperature of fouling		
		1000 °C	700 °C	500 °C
Centennial	A	1.76738	1.76738	1.76738
	w/w _b	0.0168	0.0168	0.0168
	R _{0.03} /R _{0.03b}	2.780	2.087	1.536
	T/T _b	4.217	4.217	4.217
	C _m	0.0985825	0.0985825	0.0985825
Taldinsky	A	-	1.76738	-
	w/w _b	-	0.0168	-
	R _{0.03} /R _{0.03b}	-	3.123	-
	T/T _b	-	4.217	-
	C _m	-	0.6106572	-
MHU	A	-	1.76738	-
	w/w _b	-	0.0168	-
	R _{0.03} /R _{0.03b}	-	3.565	-
	T/T _b	-	4.217	-
	C _m	-	1.429589	-

Table 6. Thermal effectiveness number by coal type and deposit temperature difference

		Deposited temperature of fouling		
		1000 °C	700 °C	500 °C
Centennial	ψ	0.769268	0.749671	0.729271
Taldinsky	ψ	-	0.378947	-
MHU	ψ	-	0.274286	-

with fouling particle size and mineral components. Consequently, their value will influence the convective heat transfer coefficient. The relationship between convective heat transfer coefficient and particle size of coal fouling is shown in Fig. 8. The convective heat transfer coefficient of centennial coal has the lowest value at 500 °C. As a result of particle size analysis, the particle size of the fouling deposited at lower temperature is the smallest. It means that convective heat transfer is related to particle size of deposit fouling. If there are many smaller particles in flue gas, the value of convective heat coefficient is decreased. When the small ash particles are agglomerated, density of deposit fouling will increase more than the big ash particles. Thus, the heat transfer efficiency decreases between flue gas and heat exchanger surface.

Fig. 9 shows the relationship between convective heat transfer coefficient and $\%(\text{Fe}_2\text{O}_3 + \text{CaO} + \text{MgO})/\%(\text{SiO}_2 + \text{Al}_2\text{O}_3)$ ratio of coal

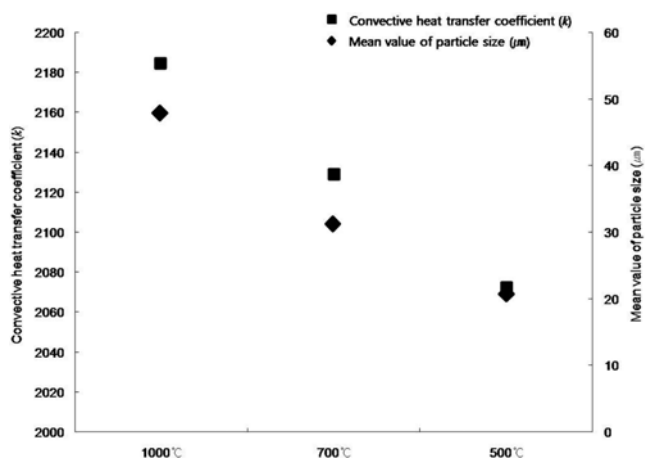


Fig. 8. Variation of convective heat transfer coefficient and particle size of coal fouling by deposited temperature (Centennial coal).

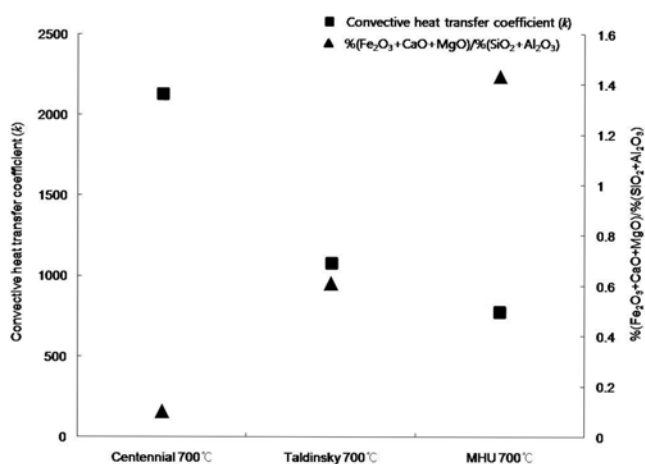


Fig. 9. Variation of convective heat transfer coefficient and % (Fe₂O₃ + CaO + MgO) / % (SiO₂ + Al₂O₃) ratio.

fouling. In the case of comparing the effect of coal types on convective heat transfer coefficient, the value of MHU coal at 700 °C is lower than Centennial and Taldinsky coal. It indicates that the value of convective heat transfer is decreased if there are more amounts of components, such as Fe₂O₃, CaO, and MgO in the coal. And active alkalis such as Fe₂O₃, CaO, and MgO lead their ash deposition rate to high value. Especially, MHU coal has many iron contents. Iron-rich particles possess a high density and have high inertia. Coalescence of pyrite with silicate minerals results in a glassy particle rich in Fe²⁺. The particles including Fe²⁺ have enough energy to adhere on deposition surface [23]. Consequently, the fouling deposition rate is increased by effect of Fe₂O₃, CaO, and MgO minerals. The value of convective heat transfer coefficient of MHU coal fouling is the lowest among samples.

CONCLUSIONS

Through the experimental investigation of characteristics of ash deposition behavior and convective heat transfer coefficient under

coal gasification condition, the results are stated below.

1) The coal fouling is deposited by two-stage deposit probe. Ash deposition rate is at 1st layer higher than at 2nd layer. It is investigated that the fouling deposited at 1st layer involves more acid mineral like SiO₂, Al₂O₃, and TiO₂ than 2nd layer from XRF result. The reason is that fouling particles shields 2nd layer and then disturbs approach of acid minerals to 2nd layer.

2) From the scanning electron microscopy (SEM), the fouling particle size of Taldinsky coal is bigger than Centennial coal fouling because of affluent presence of its alkalis like CaO, MgO, and Fe₂O₃. And from X-ray diffractometer (XRD), the fouling particle size gets to be bigger at higher temperature. It indicates that fouling particle size is substantially related to deposit temperature and ash mineral content.

3) The value of convective heat transfer coefficient is decreased due to ash deposition. Convective heat transfer coefficient has the lowest value with small particle size of coal fouling and high % (Fe₂O₃ + CaO + MgO) / % (SiO₂ + Al₂O₃) ratio.

Understanding of coal fouling characteristic is important to control operating problem of combustion or gasification system. If plant operators anticipate the problem of coal ash deposition by operating condition, they can choose the optimal coal and reduce the trouble-shooting in plant operation. And the study of convective heat transfer coefficient by ash deposition can be applied for considering optimal soot-blowing timing. Soot-blowing leads to undesirable increase of operating cost of combustion and gasification system. On the other hand, implementation of such a system in existing boilers and gasifiers requires capital costs and additional costs linked to increased fatigue of the system as a result of erosion and stresses. Finally, it is obvious that the study of cleaning optimization and fouling characteristic is of great interest.

ACKNOWLEDGEMENT

This work was supported by the project of "Development of the design technology of a Korean 300MW class IGCC demonstration plant" funded by the organization of Korea Institute of Energy Technology Evaluation and Planning (KETEP) affiliated to the Ministry of Knowledge Economy of Korean government (No. 2011951010001B).

REFERENCES

1. H. M. Shim, S. J. Lee, Y. D. Yoo, Y. S. Yun and H. T. Kim, *Korean J. Chem. Eng.*, **26**(3), 641 (2009).
2. Y. S. Yun and Y. D. Yoo, *Korean J. Chem. Eng.*, **18**(5), 679 (2001).
3. H. M. Shim, S. Y. Jung, H. Y. Wang and H. T. Kim, *Korean J. Chem. Eng.*, **26**(2), 324 (2009).
4. M. C. Van Beek, C. C. M. Rindt, J. G. Wijers and A. A. Van Steenhoven, *Heat Transfer Eng.*, **22**, 22 (2001).
5. R. W. Bryers, *Prog. Energy Combust. Sci.*, **22**, 29 (1996).
6. R. P. Gupta, T. F. Wall and L. L. Baxter, *The thermal conductivity of coal ash deposits relationships for particulate and slag structures*, in: R. P. Gupta, T. F. Wall, L. L. Baxter (Eds.), pp. 65-84, *The Impact of Mineral Impurities in Solid Fuel Combustion*, Kluwer Academic Press, New York (1999).
7. J. Wu, Y. Fang, H. Peng and Y. Wang, *Fuel Process. Technol.*, **86**, 261 (2004).

8. X. Querol, R. Juan, A. Lopez-Soler, J. L. Fernandez-Turiel and C. R. Ruiz, *Fuel*, **75**, 821 (1996).
9. S. V. Vassilev, C. G. Vassileva, A. I. Karayigit, Y. Bulut, A. Alastuey and X. Querol, *Int. J. Coal Geol.*, **61**, 65 (2005).
10. N. Moreno, X. Querol, J. M. Andres, K. Stanton, M. Towler, H. Nugteren, M. Janssen-Jurkovicová and R. Jones, *Fuel*, **84**, 1351 (2005).
11. F. Wigley and J. Williamson, *Prog. Energy Combust. Sci.*, **24**, 337 (1998).
12. H. B. Vuthaluru, J. M. Vleeskens and T. F. Wall, *Fuel Process. Technol.*, **55**, 161 (1998).
13. G. R. Couch, *Understanding slagging and fouling in of combustion*, London: IEA Coal Research (1994).
14. A. F. Skea, T. R. Bott and S. A. Beltagui, *Appl. Therm. Eng.*, **22**, 1835 (2002).
15. C. J. Geankoplis, *Transport processes and unit operation*, 3rd Ed., pp. 275-276, Prentice Hall International, Singapore (1995).
16. S. Kalisz and M. Pronobis, *Fuel*, **84**, 927 (2005).
17. M. Pronobis, *Fuel*, **85**, 474 (2006).
18. L. H. Xu, H. Namkung, H. B. Kwon and H. T. Kim, *J. Ind. Eng. Chem.*, **15**, 98 (2009).
19. K. T. Stanton, M. R. Towler, P. Mooney, R. G. Hill and X. Querol, *J. Chem. Technol. Biotechnol.*, **77**, 246 (2002).
20. X. Wu, Z. Zhang, G. Piao, X. He, Y. Chen, N. Kobayashi, S. Mori and Y. Itaya, *Energy Fuels*, **23**, 2420 (2009).
21. O. Font, X. Querol, F. Plana, P. Coca, S. Burgos and F. G. Peña, *Fuel*, **85**, 2229 (2006).
22. M. J. Fernández Llorente, J. M. Murillo Laplaza, R. Escalada Cuadrado and J. E. Carrasco García, *Fuel*, **85**, 1157 (2006).
23. L. Y. Huang, J. S. Norman, M. Pourkashanian and A. Williams, *Fuel*, **75**, 271 (1996).